

# A Model for Methylmercury Uptake and Trophic Transfer by Marine Plankton

Amina T. Schartup,<sup>\*,†,‡,§</sup> Asif Qureshi,<sup>‡,§</sup> Clifton Dassuncao,<sup>†,‡,§</sup> Colin P. Thackray,<sup>†</sup> Gareth Harding,<sup>⊥</sup> and Elsie M. Sunderland<sup>†,‡,§</sup>

<sup>†</sup>Harvard John A. Paulson School of Engineering & Applied Sciences, Harvard University, Cambridge, Massachusetts 02138, United States

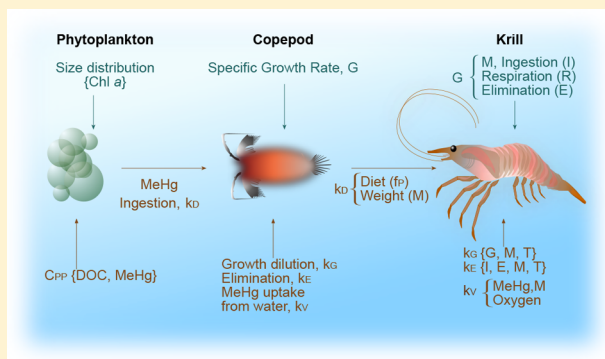
<sup>‡</sup>Department of Environmental Health, Harvard T. H. Chan School of Public Health, Harvard University, Boston, Massachusetts 02214, United States

<sup>§</sup>Department of Civil Engineering, IIT Hyderabad, Kandi, Sangareddy, TS 502285, India

<sup>⊥</sup>Bedford Institute of Oceanography, Dartmouth, NS B2Y 4A2, Canada

## Supporting Information

**ABSTRACT:** Methylmercury (MeHg) concentrations can increase by 100 000 times between seawater and marine phytoplankton, but levels vary across sites. To better understand how ecosystem properties affect variability in planktonic MeHg concentrations, we develop a model for MeHg uptake and trophic transfer at the base of marine food webs. The model successfully reproduces measured concentrations in phytoplankton and zooplankton across diverse sites from the Northwest Atlantic Ocean. Highest MeHg concentrations in phytoplankton are simulated under low dissolved organic carbon (DOC) concentrations and ultraoligotrophic conditions typical of open ocean regions. This occurs because large organic complexes bound to MeHg inhibit cellular uptake and cell surface area to volume ratios are greatest under low productivity conditions. Modeled bioaccumulation factors for phytoplankton ( $10^{2.4}$ – $10^{5.9}$ ) are more variable than those for zooplankton ( $10^{4.6}$ – $10^{6.2}$ ) across ranges in DOC (40–500  $\mu$ M) and productivities (ultraoligotrophic to hypereutrophic) typically found in marine ecosystems. Zooplankton growth dilutes their MeHg body burden, but they also consume greater quantities of MeHg enriched prey at larger sizes. These competing processes lead to lower variability in MeHg concentrations in zooplankton compared to phytoplankton. Even under hypereutrophic conditions, modeled growth dilution in marine zooplankton is insufficient to lower their MeHg concentrations, contrasting findings from freshwater ecosystems.



## INTRODUCTION

Methylmercury (MeHg) is a potent neurotoxin and oxidative stressor in humans and wildlife and is the only form of mercury (Hg) that biomagnifies in food webs.<sup>1,2</sup> Marine fish and shellfish account for more than 90% of the population wide MeHg intake in the United States.<sup>3</sup> Concentrations of MeHg in phytoplankton can be 100 000 times higher than that in seawater. However, few studies have examined how ecosystem properties affect differences in MeHg uptake and trophic transfer at the base of marine food webs.<sup>4,5</sup> Here, we develop a new model for MeHg bioaccumulation in marine phytoplankton and zooplankton.

Marine phytoplankton are thought to accumulate MeHg mainly by passive uptake from seawater (diffusion) across the cell membrane.<sup>6,7</sup> Surface area to volume ratios of phytoplankton are therefore critical for anticipating total uptake.<sup>8</sup> When ecosystems are less productive, smaller phytoplankton with greater surface area to volume ratios are

more abundant to maximize nutrient uptake efficiency, which effectively increases MeHg uptake.<sup>9,5</sup> Conversely, higher nutrient status can lead to a greater abundance of larger cells, reducing nutrient uptake at the base of the food web<sup>10</sup> and potentially also MeHg uptake.

Prior work suggests MeHg trophic transfer from phytoplankton to zooplankton is mainly driven by dietary intake with smaller direct uptake from seawater (10–20%).<sup>11</sup> Loss pathways for MeHg in zooplankton include growth dilution and temperature dependent elimination in fecal pellets.<sup>11,12</sup> Herbivorous (small) zooplankton grow most rapidly at higher temperatures and when sufficient nutrients are available.<sup>13</sup> Omnivorous (large) zooplankton are opportunistic feeders and

Received: July 26, 2017

Revised: November 8, 2017

Accepted: December 11, 2017

Published: December 11, 2017

preferentially consume the largest prey available (other smaller zooplankton) but will also consume phytoplankton, depending on availability.<sup>14</sup> Biomass dilution has been established as a major factor controlling MeHg concentrations in zooplankton from eutrophic freshwater systems.<sup>6,15</sup> Similar processes for marine ecosystems have been hypothesized but not directly observed.<sup>4</sup>

High concentrations of terrestrial dissolved organic matter may inhibit phytoplankton MeHg uptake by forming large complexes with MeHg in seawater that reduce transport across the cell membrane.<sup>16–19</sup> By contrast, higher MeHg concentrations in marine zooplankton exposed to elevated dissolved organic matter concentrations were reported in mesocosm experiments by Jonsson et al.<sup>20</sup> In these experiments, the algal community shifted from predominantly autotrophic (phytoplankton) to heterotrophic (bacterioplankton) at high dissolved organic matter concentrations. MeHg increases in zooplankton reflected lengthening of the food web rather than size based effects on phytoplankton community composition. This example illustrates why evaluating and diagnosing the role of simultaneously occurring factors that affect MeHg uptake and trophic transfer is essential for understanding differences in MeHg bioaccumulation across marine ecosystems.

Here we use experimental data and bioenergetic theory to develop a model that links ecosystem properties to MeHg uptake in phytoplankton and trophic transfer to zooplankton. Field measurements from coastal, shelf and pelagic regions of the Northwest Atlantic Ocean are used to evaluate the model. We apply the model to quantitatively bound differences in MeHg accumulation attributable to variability in primary productivity, trophic structure, and dissolved organic carbon concentrations across ecosystems.

## METHODS

**Model Overview.** We develop a nonsteady state model to calculate changes in MeHg concentrations in phytoplankton and zooplankton due to varying seawater MeHg concentrations and across different life stages for zooplankton. The model solves coupled first-order differential equations for zooplankton MeHg concentrations (wet weight) using one-step forward Euler-type numerical integration. Dissolved MeHg concentrations are used to force the simulation and can be specified deterministically or as distributions (probability density functions). Monitoring data are used to specify probability density functions for temperature, dissolved organic carbon (DOC) and chlorophyll *a* (Chl *a*) distributions in each ecosystem as input parameters that are simulated over 10<sup>3</sup> Monte Carlo iterations.

**Phytoplankton.** Our model includes three size classes of phytoplankton (picoplankton 0.2–2 μm; nanoplankton 2–20 μm; and microplankton 20–200 μm). The relative abundance of different phytoplankton size classes is based on empirical relationships with surface Chl *a* concentrations (Supporting Information (SI), Table S1).<sup>9</sup>

Phytoplankton MeHg concentrations are modeled using experimental net MeHg uptake rates from the work of Lee and Fisher<sup>5</sup> for several marine phytoplankton species. Concentrations reflect integrated uptake over 4 h, after which the cells are assumed to achieve equilibrium.<sup>5</sup> Lee and Fisher<sup>5</sup> found no relationship between MeHg uptake rates and temperature and nutrients but a strong linear correlation between cell surface area ( $S_A$ ) to volume ( $V$ ) ratios (Figure 1A; Table 1). We combine this information with data showing an exponential

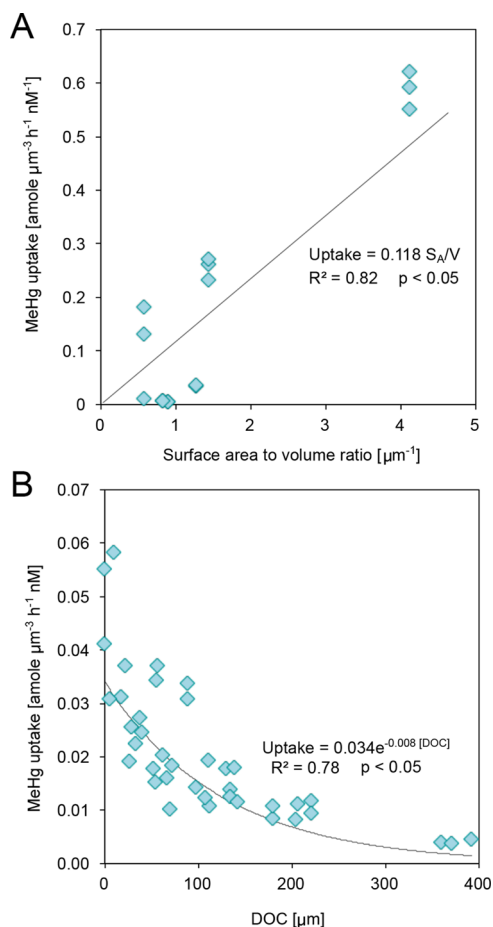


**Figure 1.** Factors affecting methylmercury (MeHg) uptake by marine phytoplankton. (A) Relationship between phytoplankton MeHg uptake rates and cell surface area to volume ratios based on experimental data reported by Lee and Fisher.<sup>5</sup> (B) Relationship between increasing dissolved organic carbon (DOC) concentrations and MeHg uptake by plankton based on data from the work of Luengen et al.<sup>17</sup>

decline in uptake ( $R^2 = 0.78$ ) with increasing DOC concentrations from the work of Luengen et al.<sup>17</sup> (Figure 1B). The resulting expression for phytoplankton MeHg uptake rate ( $U$ ) varies as a function of both cell-size and DOC concentrations in seawater (Table 1).

**Zooplankton.** We develop different model parametrizations for MeHg accumulation by herbivorous (small) and omnivorous (large) zooplankton based on established theory of growth and diet composition. For both, changes in MeHg concentrations ( $C_Z$ , ng g<sup>-1</sup>) are based on first-order rates for (1) seawater uptake ( $k_B$ , d<sup>-1</sup>), (2) dietary intake from consumed prey ( $k_D$ , d<sup>-1</sup>), (3) fecal elimination ( $k_E$ , d<sup>-1</sup>), and (4) growth dilution ( $k_G$ , d<sup>-1</sup>), as follows:

$$\frac{dC_Z}{dt} = \{k_B + k_D - (k_E + k_G)\}C_Z \quad (1)$$

Direct uptake from seawater (bioconcentration) is based on the dissolved MeHg concentration in seawater and an octanol–water partition coefficient for methylmercuric chloride (SI Table S2). Dietary assimilation efficiencies for MeHg have been shown to range between 50% and 70%<sup>11</sup> and are simulated probabilistically using a uniform distribution. MeHg elimination by zooplankton is parameterized as a function of

Table 1. Model Parameterization of Methylmercury Uptake by Marine Phytoplankton

parameter	units	description	equation or value
$C_{PP}$	$\text{ng g}^{-1}$	MeHg concentration (wet weight) in phytoplankton size class of interest	$\frac{UC_w V}{M} \times 200.59 \times 10^{-12}$
$U$	$\text{amol } \mu\text{m}^{-3} \text{ nM}^a$	empirical relationship between net MeHg uptake rate and cell surface to volume ratio	$t \frac{0.118 S_A}{V} e^{-0.008 \text{DOC}} t = 4 \text{ h}^b$
$C_W$	pM	MeHg concentration in seawater	input parameter
$\rho$	$\text{g } \mu\text{m}^{-3}$	density of phytoplankton	$10^{-12} \text{ }^7$
$V$	$\mu\text{m}^3$	volume of cell	$V = \frac{4}{3} \pi r^3$
$M$	g	wet weight of cell	$V\rho$
$r$	$\mu\text{m}$	radius of cell	
$S_A:V$	$\mu\text{m}^{-1}$	assumed surface area to volume ratio of model species of interest (spherical)	$S_A:V = 3/r$
DOC	$\mu\text{M}$	dissolved organic carbon concentration in seawater	input parameter

<sup>a</sup>amol = attomole =  $10^{-18}$  mol. <sup>b</sup>Cells reach equilibrium with seawater concentrations after 4 h.

body burden and seawater temperature (SI Table S2). Ingestion rates for all zooplankton are based on energy needed for growth and metabolic function.<sup>21</sup>

Growth is parameterized differently for herbivorous and omnivorous zooplankton. Herbivorous zooplankton growth is driven by temperature and surface productivity (Chl *a*) following the relationship developed for marine copepods by Hirst and Bunker (SI Table S2).<sup>13</sup> The composition of food consumed and associated dietary MeHg uptake is based on seawater filtration and the availability of different size classes of phytoplankton (SI Table S2).

Omnivorous (large) zooplankton growth is based on standard bioenergetics that characterize energy requirements for growth ( $G$ ,  $\text{g d}^{-1}$ , Table S3). Energy obtained from prey consumption ( $I$ ,  $\text{g g}^{-1} \text{ d}^{-1}$ , SI Tables S3 and S4) is allocated toward metabolism (respiration ( $R$ ) and elimination ( $E$ ),  $\text{g g}^{-1} \text{ d}^{-1}$ ), and the difference is used to grow:

$$G = \frac{dM}{dt} = (I - R - E)M \quad (2)$$

where  $M$  is zooplankton (g) mass and  $t$  is time (d). Species-specific von Bertalanffy growth curves from the literature are used to constrain ingestion rates needed for growth.<sup>22</sup> Omnivorous zooplankton graze primarily on herbivorous zooplankton and occasionally on large phytoplankton (microplankton).<sup>23</sup> Diet composition is weighted toward the largest available prey that falls below a predator–prey length ratio constraint derived from other studies.<sup>24–26</sup> Prey size consumed increases with length and gape size (SI Table S5).<sup>27</sup> We assume omnivorous zooplankton will preferentially consume microplankton of comparable size to copepods (<0.125 mm) due to their relative immobility.<sup>28,29</sup> The model probabilistically simulates diet composition based on zooplankton body

size and these feeding preferences. Additional details of the model parametrization are available in the SI, Table S4.

**Field Data Synthesis.** We synthesized measured concentrations of MeHg, Chl *a*, and DOC in seawater, and MeHg concentration data for phytoplankton and zooplankton from several marine ecosystems in the Northwest Atlantic margin region (Table 2). These include the Northwest Atlantic margin,<sup>30,31</sup> Long Island Sound,<sup>16,32,33</sup> and Lake Melville, an estuarine fjord in Labrador, Canada.<sup>34</sup> These marine ecosystems have varying terrestrial influences (estuarine to pelagic marine locations) and span a range of productivities, DOC concentrations and MeHg concentrations. Many studies routinely measure bulk phytoplankton MeHg concentrations that include sizes ranging from 0.2 to 200  $\mu\text{m}$  diameter. We used continuous plankton recorder data collected by Barton et al.<sup>35</sup> to characterize the cell size distribution in such samples (Figure S1) and find the mean cell diameter in the Northwest Atlantic margin region is approximately 60  $\mu\text{m}$ .

In the field, zooplankton are often separated by size rather than species or diet. While size and diet preferences are often well correlated, some large herbivorous zooplankton may be included in the omnivorous group and vice-versa during sampling. We assume small zooplankton collected in the field are mainly herbivorous and large zooplankton are mainly omnivorous. This assumption affects our model evaluation against observations rather than the model result.

## RESULTS AND DISCUSSION

**Variability in Observed Phytoplankton Methylmercury Concentrations.** Modeled and measured phytoplankton MeHg concentrations compare well ( $R^2 = 0.80$ ) across ecosystems (Figure 2A). The model successfully reproduces the approximately 100-fold variability in measured phytoplankton concentrations across sites that range from 0.005 ng

Table 2. Measured Mean MeHg Concentrations in Phytoplankton and Zooplankton

location	water	phytoplankton	zooplankton	dissolved organic carbon	chlorophyll <i>a</i>
	pM	$\text{ng g}^{-1}$	$\text{ng g}^{-1}$	$\mu\text{M}$	$\mu\text{g L}^{-1}$
Long Island Sound	0.02–0.15 <sup>a,b,c</sup>	0.01–0.5 <sup>a,b,d</sup>	0.6 <sup>b</sup>	90–250 <sup>a</sup>	1.7–24 <sup>j</sup>
NY/NJ Harbor	0.12 <sup>d</sup>	0.4 <sup>d</sup>		90–230 <sup>d</sup>	5–25 <sup>k</sup>
Lake Melville	0.04 <sup>e</sup>	0.03 <sup>e</sup>	2.7 <sup>e</sup>	200–400 <sup>e</sup>	2.7–9 <sup>l</sup>
Northwest Atlantic margin	0.01–0.03 <sup>a,f</sup>	0.06–0.14 <sup>b,f,g</sup>	0.7–2 <sup>f,g</sup>	40–100 <sup>e,h,i</sup>	0.3–3 <sup>m</sup>

<sup>a</sup>Schartup et al. (2015).<sup>16</sup> <sup>b</sup>Gosnell et al. (2017).<sup>33</sup> <sup>c</sup>Hammerschmidt et al. (2006).<sup>32</sup> <sup>d</sup>Balcom et al. (2008).<sup>42</sup> <sup>e</sup>Schartup et al. (2015).<sup>34</sup> <sup>f</sup>Hammerschmidt et al. (2013).<sup>31</sup> <sup>g</sup>Harding et al. (2005).<sup>30</sup> <sup>h</sup>Balch et al. (2016).<sup>43</sup> <sup>i</sup>Vlahos et al. (2002).<sup>44</sup> <sup>j</sup>LISS Water Quality Monitoring Program,<sup>45</sup> Chl *a* from 1991 to 2011. <sup>k</sup>Bloomberg and Strickland (2011),<sup>46</sup> Chl *a* from 1986 to 2012. <sup>l</sup>NASA Goddard Space Flight Center (2014),<sup>47</sup> Chl *a* from 2002 to 2012. <sup>m</sup>World Ocean Database,<sup>48</sup> Chl *a* from 1980 to 2015.

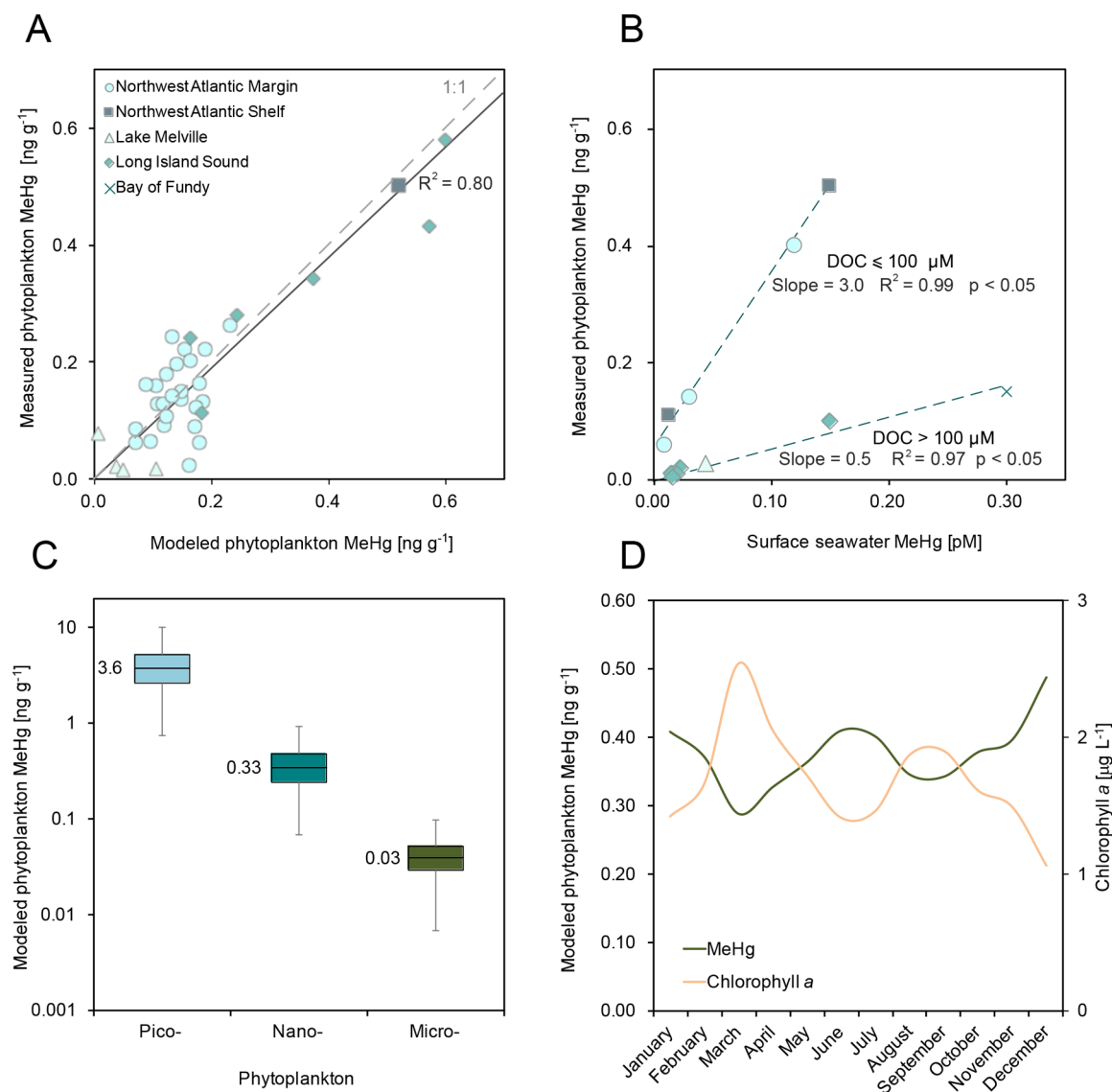


**Figure 2.** Modeled and measured phytoplankton methylmercury (MeHg) concentrations. (A) Modeled and measured concentrations across ecosystems. (B) Mean measured phytoplankton MeHg concentrations per location or study as function of seawater MeHg levels and approximate dissolved organic carbon (DOC) concentration. (C) Variability in modeled phytoplankton MeHg concentrations in the Northwest Atlantic margin across the three size classes considered here. (D) Modeled bulk phytoplankton MeHg concentration during a typical year in the Northwest Atlantic margin in response to changing productivity and phytoplankton size fractions. Monthly average chlorophyll *a* (Chl *a*) concentrations are derived from measurements in the Northwest Atlantic margin for the same time period as the phytoplankton MeHg data (1997–2001).<sup>49–51</sup>

$\text{g}^{-1}$  in Long Island Sound to greater than  $0.5 \text{ ng g}^{-1}$  on the Northwest Atlantic shelf. This variability is larger than the range in seawater MeHg concentrations (approximately 30-fold), illustrating the role of other ecological properties in enhancing or reducing MeHg uptake in phytoplankton. The ability of the model to capture variability in field measurements suggests seawater MeHg, DOC, and cell size are the main drivers of phytoplankton MeHg concentrations across ecosystems.

Across ecosystems, measured phytoplankton concentrations are linearly related to measured seawater MeHg concentrations, but the slope of the relationship changes with seawater DOC concentrations (Figure 2B). At relatively higher DOC concentrations that exceed  $100 \mu\text{M}$  (Long Island Sound, the Bay of Fundy, and Lake Melville Labrador) a smaller fraction of MeHg is taken up by phytoplankton and the slope of the relationship with MeHg is thus shallower. These sites are

estuarine locations more highly influenced by terrestrial organic matter inputs, which has been shown in other work to effectively reduce MeHg transport across the cell membrane.<sup>16,36</sup> Relatively lower DOC concentrations ( $<100 \mu\text{M}$ ) are found on the Northwest Atlantic margin and shelf (Figure 2B). At similar seawater MeHg concentrations, phytoplankton from these offshore regions are approximately 4-fold higher than those from estuarine locations high in DOC (Figure 2B).

Separating phytoplankton into size fractions of sufficient mass for MeHg analysis is technically challenging, and this is particularly true for open ocean collections. Thus, most studies collect and report bulk phytoplankton (seston) MeHg concentrations that represent the sum product of MeHg in different phytoplankton size classes filterable from seawater below  $200 \mu\text{m}$  diameter.<sup>31,33</sup> Figure 2C shows 100-fold variability in modeled phytoplankton MeHg concentrations

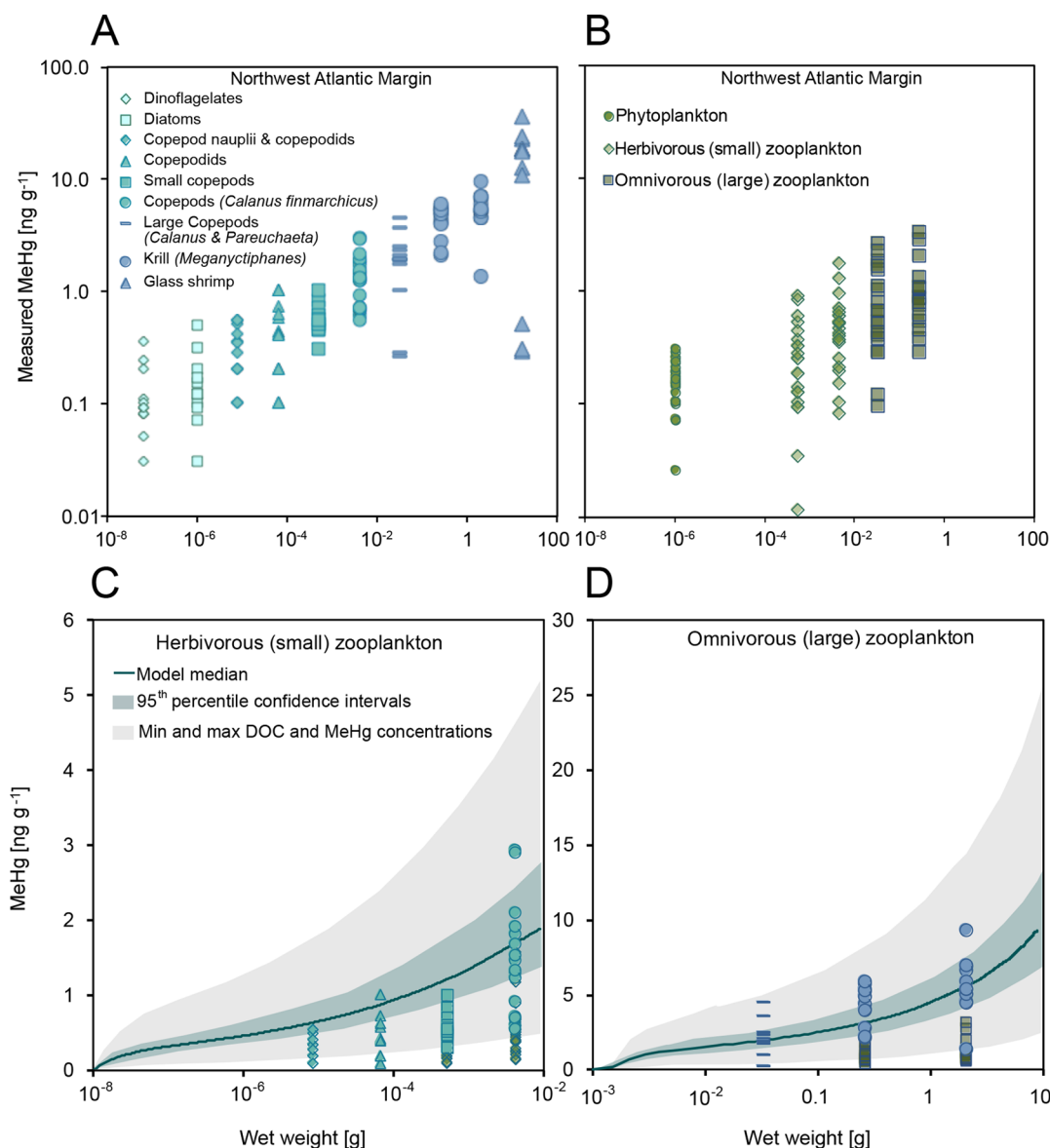


**Figure 3.** Modeled and measured methylmercury (MeHg) concentrations in phytoplankton and zooplankton from the Northwest Atlantic margin. (A) Samples from the work of Harding et al.<sup>30</sup> were sorted by size and species (SI Table S6). (B) Samples from the work of Hammerschmidt et al.<sup>31</sup> were sorted by size. (C and D) Modeled (SI Table S7) and measured zooplankton MeHg concentrations with measurements from the works of Harding et al.<sup>30</sup> and Hammerschmidt et al.<sup>31</sup> indicated by symbols matching those from panels A and B. Shaded regions for panels C and D indicate 95th percentile confidence intervals from probabilistic simulations (green) based on variable assimilation efficiencies and diet composition and minimum–maximum results seawater dissolved organic carbon (DOC) and MeHg (gray) concentrations. Ranges in MeHg and DOC are based on concentrations measured in the Northwest Atlantic margin (Table 2).

from the Northwest Atlantic margin (Table 2) across the three size classes considered. Mean MeHg concentrations are 0.03 ng g<sup>-1</sup> in the largest size class (microplankton) modeled compared to 3.6 ng g<sup>-1</sup> in the smallest size class (picoplankton). Greater surface area to volume ratios in smaller cells allows for increased uptake of MeHg per gram of cell, resulting in MeHg cell content inversely related to cell size. This is consistent with what is observed for nutrient uptake.<sup>37</sup> However, unlike nutrients that are consumed by metabolic processes, MeHg binds to protein and accumulates in the cell.

Ecosystem productivity affects the size distribution of algal cells and associated bulk MeHg concentration measurable in field samples. Model results shown in Figure 2D show greater than 50% variability in bulk phytoplankton MeHg concen-

trations (weighted by size distribution) across different months due to annual variability in primary productivity in the Northwest Atlantic margin (Figure 2D). These changes are smaller than differences across size classes shown in Figure 2C because the algal community at any given time represents a mixture of different cell sizes rather than exclusive domination by a single size fraction (SI Figure S2).

**Observed Zooplankton Methylmercury Concentrations.** Measured MeHg concentrations in phytoplankton and zooplankton from the Northwest Atlantic margin are shown in Figures 3A and B. Data in Figure 3A from Harding et al.<sup>30</sup> were separated by species and show characteristic MeHg biomagnification with increasing size of marine plankton. As expected, juvenile copepod species (herbivorous) have lower MeHg levels than adult copepods, krill, and glass shrimp

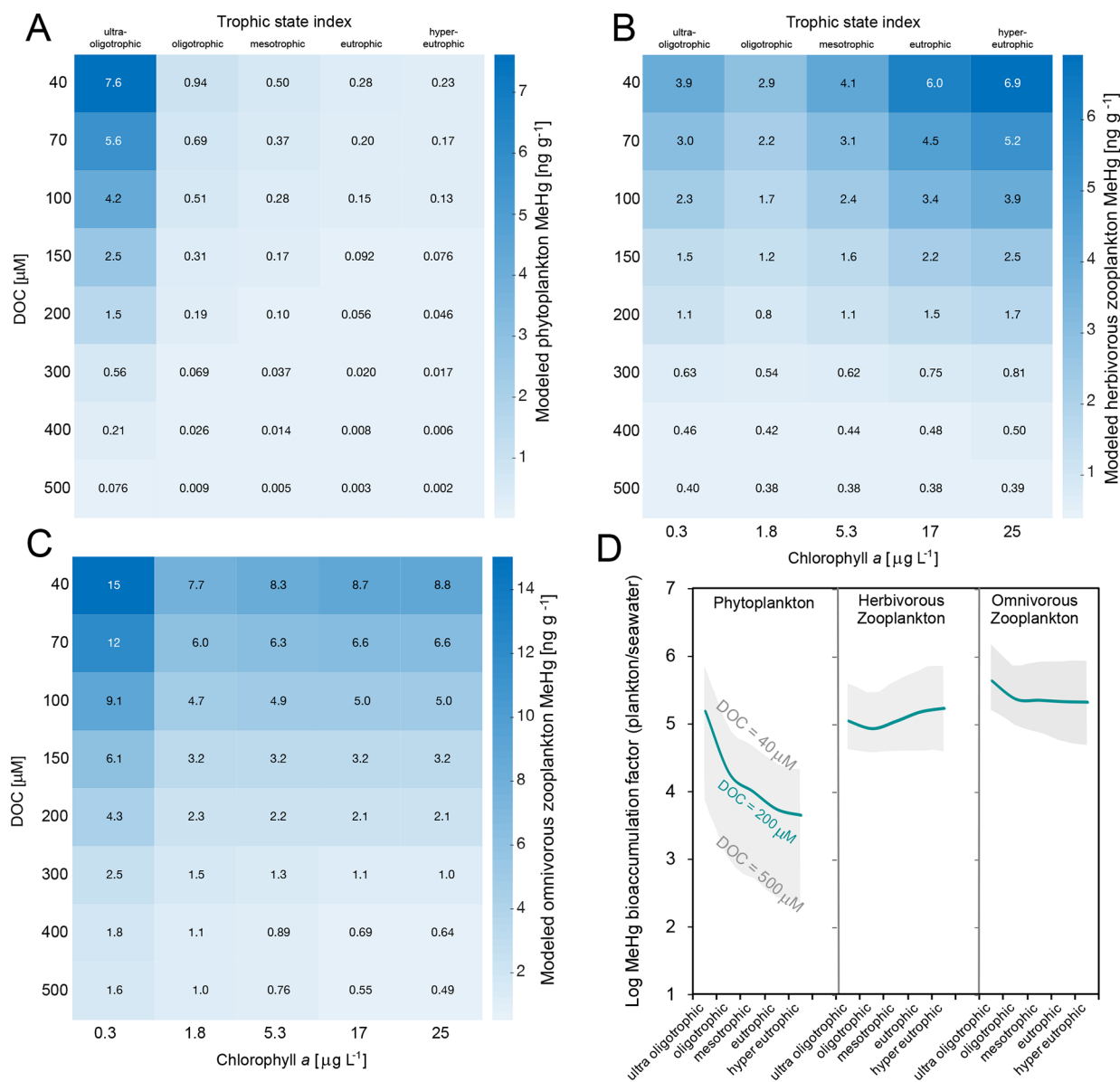


**Figure 4.** Modeled impacts of dissolved organic carbon (DOC) and productivity on methylmercury (MeHg) accumulation in phytoplankton and zooplankton in the Northwest Atlantic region. Panels (A–C) Modeled MeHg concentrations in bulk phytoplankton, and herbivorous and omnivorous zooplankton for seawater MeHg concentrations of 50 fM and variable DOC and chlorophyll *a* (Chl *a*) across the ranges shown in Table 2. (D) Modeled shifts in bioaccumulation factors (plankton MeHg/seawater MeHg) with changing trophic state and DOC. Median seawater DOC of 200  $\mu\text{M}$  is shown as the solid line with ranges between 40 and 500  $\mu\text{M}$  shown as shaded gray regions.

(omnivorous). Many studies separate plankton by size rather than species, as shown for example in Figure 3B based on data from Hammerschmidt et al.<sup>31</sup> from the same region. Size fractionated data are more likely to contain species at multiple trophic levels and abiotic particles, resulting in greater variability in measured concentrations. MeHg biomagnification in small and large zooplankton relative to phytoplankton is apparent in both data sets.

Figure 3C and D show modeled medians and ranges for MeHg concentrations in herbivorous (small) and omnivorous (large) zooplankton in the Northwest Atlantic margin based on ecosystem properties shown in Table 2. Characteristic increases in MeHg with increasing zooplankton weight are apparent for both small and large modeled species, which is similar to field observations shown in Figure 3A and B. We find 70% of small (herbivorous) zooplankton ( $n = 97$ ) and 75% of

large (omnivorous) zooplankton ( $n = 71$ ) measurements fall within the bounds of model simulations (min–max). For data from Harding et al.<sup>30</sup> that are separated by species, 83% of small (herbivorous) zooplankton ( $n = 53$ ) and 95% of large (omnivorous) zooplankton ( $n = 37$ ) fall within model bounds. Ranges in MeHg concentrations due to stochasticity in diet and MeHg assimilation efficiencies are shown as the darker color around the median in Figure 3C and D. Larger variability due to observed ranges in seawater MeHg and DOC concentrations are shown as the lighter gray outer shaded regions in Figure 3C and D.

Zooplankton tissue burdens reflect the balance between intake and loss processes over their lifespan. Extracting intake values from the model, we calculate that, for both herbivorous and omnivorous zooplankton, more than 80% of their MeHg is from dietary ingestion and the remainder is direct uptake from

seawater. This is similar to experimental findings previously reported.<sup>11</sup>

**Modeled Impacts of Productivity and DOC on Bioaccumulation.** Figure 4 shows modeled planktonic MeHg concentrations across the range of seawater DOC concentrations and trophic states typically found in Northwest Atlantic marine regions. Chl *a* concentrations corresponding to trophic states ranging from ultraoligotrophic to hypereutrophic and a mean seawater MeHg concentration held constant at 50 fM (Table 2) were used to force the bioaccumulation model. Results show variability in phytoplankton MeHg concentrations (bioaccumulation factors BAFs =  $10^{2.4}$ – $10^{5.9}$ ) are much larger than for herbivorous zooplankton (BAFs =  $10^{4.6}$ – $10^{5.8}$ ) and omnivorous zooplankton (BAFs =  $10^{4.7}$ – $10^{6.2}$ ), as discussed further below.

Figure 4A shows lowest modeled phytoplankton MeHg concentrations ( $0.002 \text{ ng g}^{-1}$ ) are found under hypereutrophic conditions and  $500 \mu\text{M}$  DOC concentrations, while highest levels ( $7.6 \text{ ng g}^{-1}$ ) occur at  $40 \mu\text{M}$  DOC and ultraoligotrophic conditions. Under ultraoligotrophic conditions and  $\text{DOC} < 200 \mu\text{M}$ , phytoplankton MeHg concentrations exceed or are comparable to those of herbivorous zooplankton (Figure 4B).

Differences in phytoplankton MeHg across trophic state indices range from 33- to 38-fold and reflect the decline in cell surface area to volume ratios in higher productivity ecosystems (Figure 4A). Figure 4A/D shows a nonlinear decline in phytoplankton MeHg at higher productivities. The steepest decline occurs between ultraoligotrophic and oligotrophic ecosystems characteristic of many pelagic regions of the ocean. This suggests changes in the nutrient status of the lowest productivity regions of the ocean due to climate driven shifts in circulation or anthropogenic nutrient inputs<sup>38</sup> may have the largest direct impacts on phytoplankton MeHg concentrations. We find phytoplankton MeHg concentrations vary by 100-fold across the range of DOC considered here. This is greater than differences attributable to shifts in ecosystem productivity suggesting DOC may be more important than trophic status for variability in phytoplankton MeHg concentrations across ecosystems (Figure 4A).

For herbivorous zooplankton (Figure 4B), changes in MeHg concentrations across trophic state reflect the balance between accumulation due to ingestion and growth dilution. Herbivorous zooplankton consume more and grow faster at higher nutrient concentrations. Their dietary MeHg content depends on phytoplankton MeHg content and ingestion rates. The decline in herbivorous zooplankton MeHg concentrations between ultraoligotrophic and oligotrophic conditions (Figure 4B, D) is driven by differences in phytoplankton MeHg content, which are highest at low nutrient concentrations (Figure 4A, D). For mesotrophic to hypereutrophic conditions, the increase in food availability and MeHg intake is not fully offset by increases in growth, resulting in an increase in concentrations (Figure 4B, D). This is most pronounced at low DOC concentrations characteristic of more open ocean regions.

Variable DOC concentrations have a relatively larger influence on herbivorous zooplankton MeHg concentrations (factor of 10–18-fold variability) than trophic state index (Figure 4C). In low DOC environments, modeling results suggest herbivorous zooplankton MeHg concentrations will vary by slightly more than a factor of 2 between ultraoligotrophic and hypereutrophic conditions. This is much smaller than the range in phytoplankton MeHg concentrations.

At the highest DOC concentrations, trophic state variability has almost no impact on herbivorous zooplankton concentrations. In freshwater ecosystems growth dilution of zooplankton MeHg has been widely reported.<sup>6,15</sup> For marine ecosystems, we find for both phytoplankton and herbivorous zooplankton that DOC may be more important than trophic status for differences in MeHg content across sites.

Changes in omnivorous zooplankton MeHg concentrations across DOC and trophic state index are of a similar magnitude to those for herbivorous zooplankton, and relatively smaller than for phytoplankton (Figure 4C). For omnivorous zooplankton, there is an approximately 10-to-18-fold decline in MeHg concentrations across DOC concentrations. Concentrations of MeHg decline in omnivorous zooplankton as the system shifts from ultraoligotrophic to oligotrophic but remain relatively stable across further increases in nutrient status. This suggests additional intake of MeHg at higher productivity is balanced somewhat equally by growth between oligotrophic and hypereutrophic states.

**Implications for Ecosystem Change.** Climate driven changes are increasing terrestrial discharges containing both DOC and nutrients to many marine ecosystems, particularly in northern areas.<sup>39</sup> Across ecosystems, model results suggest impacts of shifts in nutrient status and productivity will be most pronounced for phytoplankton MeHg concentrations. The model shows (Figure 4D) that DOC and higher productivity can result in a more than 3 orders of magnitude decline in phytoplankton MeHg concentrations. However, this variability is dampened following trophic transfer to zooplankton due to the competing influences of growth dilution and increased dietary ingestion of MeHg as zooplankton body size increases.

Prior work has hypothesized based on research from freshwater ecosystems<sup>6,15</sup> that growth dilution in more productive marine ecosystems will lead to lower MeHg levels in marine food webs.<sup>4</sup> Our model also shows that higher productivity results in lower phytoplankton MeHg concentrations, but we find that this effect does not propagate to higher trophic levels. Thus, shifts in trophic state index have a relatively small direct impact on trophic transfer of MeHg to zooplankton compared to increases in DOC concentrations (Figure 4). Increased nutrients and DOC in marine ecosystems can also enhance MeHg production, which propagates through the food web.<sup>16,34,40,41</sup> Field data and modeling results presented here suggests MeHg concentrations at the base of the marine food web will change linearly with seawater MeHg concentrations, and are propagated to higher trophic level species.

## ■ ASSOCIATED CONTENT

### 📄 Supporting Information

The Supporting Information is available free of charge on the ACS Publications website at DOI: 10.1021/acs.est.7b03821.

Additional information on model parametrization and plankton data are included in 7 tables and 2 figures (PDF)

## ■ AUTHOR INFORMATION

### Corresponding Author

\*Mailing address: 29 Oxford Street, Cambridge, MA 02138. E-mail: [schartup@hsph.harvard.edu](mailto:schartup@hsph.harvard.edu)

ORCID 

Amina T. Schartup: 0000-0002-9289-8107

Clifton Dassuncao: 0000-0001-7140-1344

Elsie M. Sunderland: 0000-0003-0386-9548

## Notes

The authors declare no competing financial interest.

## ACKNOWLEDGMENTS

We acknowledge financial support for this work from the U.S. National Science Foundation (OCE 1260464) and the U.S. Environmental Protection Agency contract EP-H-11-001346.

## REFERENCES

- (1) Grandjean, P.; Satoh, H.; Murata, K.; Eto, K. Adverse effects of methylmercury: Environmental health research implications. *Environ. Health Perspect.* **2010**, *118*, 1137–1145.
- (2) Wiener, J. G.; Krabbenhoft, D. P.; Heinz, G. H.; Scheuhammer, A. M. Ecotoxicology of mercury. In *Handbook of ecotoxicology*; CRC Press: Boca Raton, FL, 2003; pp. 409–463.
- (3) Sunderland, E. M. Mercury exposure from domestic and imported estuarine and marine fish in the U.S. seafood market. *Environ. Health Perspect.* **2006**, *115*, 235–242.
- (4) Driscoll, C. T.; Chen, C. Y.; Hammerschmidt, C. R.; Mason, R. P.; Gilmour, C. C.; Sunderland, E. M.; Greenfield, B. K.; Buckman, K. L.; Lamborg, C. H. Nutrient supply and mercury dynamics in marine ecosystems: A conceptual model. *Environ. Res.* **2012**, *119*, 118–131.
- (5) Lee, C.-S.; Fisher, N. S. Methylmercury uptake by diverse marine phytoplankton. *Limnol. Oceanogr.* **2016**, *61*, 1626–1639.
- (6) Pickhardt, P. C.; Fisher, N. S. Accumulation of inorganic and methylmercury by freshwater phytoplankton in two contrasting water bodies. *Environ. Sci. Technol.* **2007**, *41*, 125–131.
- (7) Mason, R. P.; Reinfelder, J. R.; Morel, F. M. M. Uptake, Toxicity, and Trophic Transfer of Mercury in a Coastal Diatom. *Environ. Sci. Technol.* **1996**, *30*, 1835–1845.
- (8) Fisher, N. S. S. Accumulation of metals by marine picoplankton. *Mar. Biol.* **1985**, *87*, 137–142.
- (9) Uitz, J.; Claustre, H. H.; Morel, A. A.; Hooker, S. B. Vertical distribution of phytoplankton communities in open ocean: An assessment based on surface chlorophyll. *J. Geophys. Res.* **2006**, *111*, C08005.
- (10) Hein, M.; Pedersen, M.; Sand-Jensen, K. Size-dependent nitrogen uptake in micro- and macroalgae. *Mar. Ecol.: Prog. Ser.* **1995**, *118*, 247–253.
- (11) Lee, C.-S.; Fisher, N. S. Bioaccumulation of methylmercury in a marine copepod. *Environ. Toxicol. Chem.* **2017**, *36*, 1287–1293.
- (12) Arnot, J. A.; Gobas, F. F. A. P. C. A food web bioaccumulation model for organic chemicals in aquatic ecosystems. *Environ. Toxicol. Chem.* **2004**, *23*, 2343–2355.
- (13) Hirst, A. G.; Bunker, A. J. Growth of Marine Planktonic Copepods: Global Rates and Patterns in Relation to Chlorophyll a, Temperature, and Body Weight. *Limnol. Oceanogr.* **2003**, *48*, 1988–2010.
- (14) Blachowiak-Samolyk, K.; Kwasniewski, S.; Dmoch, K.; Hop, H.; Falk-Petersen, S. Trophic structure of zooplankton in the Fram Strait in spring and autumn 2003. *Deep Sea Res., Part II* **2007**, *54*, 2716–2728.
- (15) Karimi, R.; Chen, C. Y.; Pickhardt, P. C.; Fisher, N. S.; Folt, C. L. Stoichiometric controls of mercury dilution by growth. *Proc. Natl. Acad. Sci. U. S. A.* **2007**, *104*, 7477–7482.
- (16) Schartup, A. T.; Ndu, U. C.; Balcom, P. H.; Mason, R. P.; Sunderland, E. M. Contrasting Effects of Marine and Terrestrially Derived Dissolved Organic Matter on Mercury Speciation and Bioavailability in Seawater. *Environ. Sci. Technol.* **2015**, *49*, 5965–5972.
- (17) Luengen, A. C.; Fisher, N. S.; Bergamaschi, B. a. Dissolved organic matter reduces algal accumulation of methylmercury. *Environ. Toxicol. Chem.* **2012**, *31*, 1712–1719.
- (18) Zhong, H.; Wang, W.-X. Controls of dissolved organic matter and chloride on mercury uptake by a marine diatom. *Environ. Sci. Technol.* **2009**, *43*, 8998–9003.
- (19) Lee, C.-S.; Fisher, N. S. Bioaccumulation of methylmercury in a marine diatom and the influence of dissolved organic matter. *Mar. Chem.* **2017**, *197*, 70.
- (20) Jonsson, S.; Andersson, A.; Nilsson, M. B.; Skjllberg, U.; Lundberg, E.; Schaefer, J. K.; Åkerblom, S.; Björn, E.; et al. Terrestrial discharges mediate trophic shifts and enhance methylmercury accumulation in estuarine biota. *Sci. Adv.* **2017**, *3*, e1601239.
- (21) Kleppel, G. S. On the diets of calanoid copepods. *Mar. Ecol.: Prog. Ser.* **1993**, *99*, 183–195.
- (22) von Bertalanffy, L. A quantitative theory of organic growth (Inquiries on growth laws. II). *Hum. Biol.* **1938**, *10*, 181–213.
- (23) Turner, J. T. The Importance of Small Pelagic Planktonic Copepods and Their Role in Pelagic Marine Food Webs. *Zool. Stud.* **2004**, *43*, 255–266.
- (24) Scharf, F. S.; Juanes, F.; Rountree, R. a. Predator size - Prey size relationships of marine fish predators: Interspecific variation and effects of ontogeny and body size on trophic-niche breadth. *Mar. Ecol.: Prog. Ser.* **2000**, *208*, 229–248.
- (25) Barnes, C.; Maxwell, D.; Reuman, D.; Jennings, S. Global patterns in predator – prey size relationships reveal size dependency of trophic transfer efficiency. *Ecology* **2010**, *91*, 222–232.
- (26) Bautista, B.; Harris, R. P. Copepod gut contents, ingestion rates and grazing impact on phytoplankton in relation to size structure of zooplankton and phytoplankton during a spring bloom. *Mar. Ecol.: Prog. Ser.* **1992**, *82*, 41–50.
- (27) Nilsson, P. A.; Brönmark, C. Prey vulnerability to a gape-size limited predator: Behavioural and morphological impacts on northern pike piscivory. *Oikos* **2000**, *88*, 539–546.
- (28) Lass, S.; Tarling, G. A.; Virtue, P.; Matthews, J. B. L.; Mayzaud, P.; Buchholz, F. On the food of northern krill *Meganctiphanes norvegica* in relation to its vertical distribution. *Mar. Ecol.: Prog. Ser.* **2001**, *214*, 177–200.
- (29) Bunn, S. E.; Arthington, A. H. Basic Principles and Ecological Consequences of Altered Flow Regimes for Aquatic Biodiversity. *Environ. Manage.* **2002**, *30*, 492–507.
- (30) Harding, G.; Dalziel, J.; Vaas, P. Prevalence and bioaccumulation of methyl mercury in the food web of the Bay of Fundy, Gulf of Maine. In *The changing Bay of Fundy: Beyond 400 years. Proceedings of the 6th Bay of Fundy workshop, Cornwallis, Nova Scotia, Set 29–Oct 2, 2004. Environment Canada–Atlantic Region*, Percy, J. A., Evans, A. J., Welles, P. G., Rolston, S. J., Eds.; 2005; pp 76–77.
- (31) Hammerschmidt, C. R.; Finiguerra, M. B.; Weller, R. L.; Fitzgerald, W. F. Methylmercury accumulation in plankton on the continental margin of the northwest Atlantic Ocean. *Environ. Sci. Technol.* **2013**, *47*, 3671–3677.
- (32) Hammerschmidt, C. R. C. C. R.; Fitzgerald, W. F. W. Bioaccumulation and trophic transfer of methylmercury in Long Island Sound. *Arch. Environ. Contam. Toxicol.* **2006**, *51*, 416–424.
- (33) Gosnell, K. J.; Balcom, P. H.; Tobias, C. R.; Gilhooly, W. P.; Mason, R. P. Spatial and temporal trophic transfer dynamics of mercury and methylmercury into zooplankton and phytoplankton of Long Island Sound. *Limnol. Oceanogr.* **2017**, *62*, 1122–1138.
- (34) Schartup, A. T.; Balcom, P. H.; Soerensen, A. L.; Gosnell, K. J.; Calder, R. S. D.; Mason, R. P.; Sunderland, E. M. Freshwater discharges drive high levels of methylmercury in Arctic marine biota. *Proc. Natl. Acad. Sci. U. S. A.* **2015**, *112*, 11789–11794.
- (35) Barton, A. D.; Finkel, Z. V.; Ward, B. A.; Johns, D. G.; Follows, M. J. On the roles of cell size and trophic strategy in North Atlantic diatom and dinoflagellate communities. *Limnol. Oceanogr.* **2013**, *58*, 254–266.
- (36) Ndu, U.; Mason, R. P.; Zhang, H.; Lin, S.; Visscher, P. T. Effect of inorganic and organic ligands on the bioavailability of methylmercury as determined by using a mer-lux bioreporter. *Appl. Environ. Microbiol.* **2012**, *78*, 7276–7282.
- (37) Chisholm, S. W. Phytoplankton Size. *Prim. Product. Biogeochem. Cycles Sea* **1992**, *2139*, 213–237.



(38) Townsend, D. W.; Rebeck, N. D.; Thomas, M. A.; Karp-Boss, L.; Gettings, R. M. A changing nutrient regime in the Gulf of Maine. *Cont. Shelf Res.* **2010**, *30*, 820–832.

(39) Balch, W.; Drapeau, D.; Bowler, B.; Huntington, T. Step-changes in the physical, chemical and biological characteristics of the Gulf of Maine, as documented by the GNATS time series. *Mar. Ecol.: Prog. Ser.* **2012**, *450*, 11–35.

(40) Soerensen, A. L. L.; Schartup, A. T. T.; Skrobonja, A.; Björn, E. Organic matter drives high interannual variability in methylmercury concentrations in a subarctic coastal sea. *Environ. Pollut.* **2017**, *229*, 531–538.

(41) Soerensen, A. L.; Schartup, A. T.; Gustafsson, E.; Gustafsson, B. G.; Undeman, E.; Björn, E. Eutrophication Increases Phytoplankton Methylmercury Concentrations in a Coastal Sea—A Baltic Sea Case Study. *Environ. Sci. Technol.* **2016**, *50*, 11787–11796.

(42) Balcom, P. H.; Hammerschmidt, C. R.; Fitzgerald, W. F.; Lamborg, C. H.; O'Connor, J. S. Seasonal distributions and cycling of mercury and methylmercury in the waters of New York/New Jersey Harbor Estuary. *Mar. Chem.* **2008**, *109*, 1–17.

(43) Balch, W.; Huntington, T.; Aiken, G.; Drapeau, D.; Bowler, B.; Lubelczyk, L.; Butler, K. Toward a quantitative and empirical dissolved organic carbon budget for the Gulf of Maine, a semienclosed shelf sea. *Global Biogeochem. Cycles* **2016**, *30*, 268–292.

(44) Vlahos, P.; Chen, R. F.; Repeta, D. J. Dissolved organic carbon in the Mid-Atlantic Bight. *Deep Sea Res., Part II* **2002**, *49*, 4369–4385.

(45) CTDEEP. Long Island Sound Study Water Quality Monitoring Program. <http://longislandsoundstudy.net/> (accessed Jun 7, 2017).

(46) Bloomberg, M. R.; Strickland, C. H. *New York Harbor Water Quality Report*; 2011.

(47) Nasa Goddard Space Flight Center. Moderate resolution imaging spectroradiometer (MODIS) aqua ocean color data; 2014 reprocessing. <https://oceancolor.gsfc.nasa.gov/reprocessing/r2014/aqua/> (accessed Dec 2017).

(48) Boyer, T. P.; Antonov, J. I.; Baranova, O. K.; Garcia, H. E.; Johnson, D. R.; Mishonov, A. V.; O'Brien, T. D.; Seidov, D.; Smolyar, I.; Zweng, M. M.; Paver, C. R.; Locarnini, R. A.; Reag, S. *World Ocean Database 2013*, NOAA Atlas NESDIS 72; Silver Spring, MD, 2013.

(49) Fisheries and Oceans Canada. *2005 State of the ocean: chemical and biological oceanographic conditions in the Gulf of Maine—Bay of Fundy, Scotian Shelf and the Southern Gulf of St. Lawrence*; Canadian Science Advisory Secretariat Science Advisory Report 2006/048; 2007.

(50) Hyde, K. J. W. W.; O'Reilly, J. E.; Oviatt, C. A. Validation of SeaWiFS chlorophyll a in Massachusetts Bay. *Cont. Shelf Res.* **2007**, *27*, 1677–1691.

(51) Thomas, A. C.; Townsend, D. W.; Weatherbee, R. Satellite-measured phytoplankton variability in the Gulf of Maine. *Cont. Shelf Res.* **2003**, *23*, 971–989.